

1 CHEN, X., MCGOWAN, S., XIAO, X., STEVENSON, M.A. and YANG, X., 2018. Direct and indirect
2 effects of Holocene climate variations on catchment and lake processes of a treeline lake, SW
3 China Palaeogeography, Palaeoclimatology, Palaeoecology. 502, 119–129
4 <https://doi.org/10.1016/j.palaeo.2018.04.027>

5

6

7 **Direct and indirect effects of Holocene monsoonal variations on catchment and**
8 **lake processes of a treeline lake, SW China**

9

10 Xu Chen^{1*}, Suzanne McGowan², Xiayun Xiao³, Mark A. Stevenson⁴, Xiangdong
11 Yang³, Yanling Li³, Enlou Zhang³

12

13 1 State Key Laboratory of Biogeology and Environmental Geology, School of Earth
14 Sciences, China University of Geosciences, Wuhan, China

15 2 School of Geography, University of Nottingham, Nottingham NG7 2RD, UK

16 3 State Key Laboratory of Lake Science and Environment, Nanjing Institute of
17 Geography and Limnology, Chinese Academy of Sciences, Nanjing, China

18 4 School of Natural and Environmental Sciences, Newcastle University, Newcastle-
19 upon-Tyne, UK

20

21 *Corresponding author; e-mail address: xuchen@cug.edu.cn

22 **Abstract:** Sedimentary records of inorganic elements and pigments over the last
23 ~12,000 cal. yr BP are used to assess major changes in limnological conditions of
24 Tiancai Lake (a small treeline lake, SW China), in response to Holocene monsoonal
25 variations. Primary producer communities shifted from cyanobacteria and
26 cryptophytes in the early Holocene, towards siliceous algae in the mid-Holocene
27 and chlorophytes/ aquatic plants in the late Holocene. Algae responded to a
28 combination of climate-mediated vegetation and soil development associated with
29 allochthonous inputs of dissolved nutrients and organic matter, and lake sediment
30 infilling. General decreases in Al, Pb, Cu and Zn from the early Holocene probably
31 resulted from soil podsolization and the sequestration of these elements within soils.
32 Changes in Mn and Fe were likely linked to redox condition dynamics in catchment
33 soils and water column. Synchronous peaks in Ti, Ba, Ca, Sr, Na, K and Mg, median
34 grain size and magnetic susceptibility coincided with the troughs in the chemical
35 index of alteration, indicating that episodic cold events enhanced upland bedrock
36 erosion and transported unleached and coarse detritus into the lake. These cold
37 events broadly correlate with the ice-rafting events in the North Atlantic. Although
38 Holocene cold events altered the influx of minerogenic elements by regulating
39 upland bedrock erosion, climate-mediated vegetation and soil development led to a
40 muted impact on primary producers. Holocene algal community shifts were subtle,
41 reflecting the relative abundance of P (derived from weathering) and N (derived
42 from soils) throughout the record, with the most marked effects on the lake biota
43 being benthic expansion which occurred in response to sediment infilling.

44

45 **Keywords:** Holocene monsoonal variations; Lake sediment; Pigments; Inorganic

46 elements; Alpine lake; Lake ontogeny

47

48 **1. Introduction**

49 Treeline lakes located close to ecotonal boundaries are highly sensitive to climate
50 change as small variations in climate can give rise to large transitions in catchment
51 vegetation and runoff, thereby influencing lake functioning (Battarbee et al., 2002;
52 Lotter and Birks, 2003; Catalan et al., 2013). In alpine/boreal environments, long-
53 term catchment development and ontogeny generally cause lakes to become acidic
54 and dilute, as the influx of organic matter increases and mineral leaching declines
55 with soil development (Engstrom et al., 2000; Fritz et al., 2004; Fritz and Anderson,
56 2013; Lu et al., 2017). Given that key nutrients (phosphorus and bases such as Ca)
57 for alpine lakes come largely from bedrock weathering (Boyle et al., 2013), mineral
58 depletion after glacial retreat can trigger ecosystem succession (Engstrom et al.,
59 2000). Generally, the initial alkaliphilous diatom species of the late-glacial are
60 replaced by acidophilous taxa in boreal lakes (Pennington et al., 1972; Renberg,
61 1990; Bradshaw et al., 2000).

62 Alpine lakes in southwestern China, close to the Tibetan Plateau, are strongly
63 influenced by the Asian monsoon. Sedimentary records in these lakes can provide
64 long-term insights into past climate dynamics over Southeast Asia (Xiao et al., 2014;
65 Wang et al., 2016a; Zhang et al., 2017; Li et al., 2018), with important socio-
66 economic or environmental ramifications (Overpeck et al., 1996). Generally, the
67 weak Asian monsoon during the late-glacial was replaced by a more intensified
68 monsoon after the onset of the Holocene. Warm and wet conditions persisted until
69 ca. 4.5-5.0 ka BP when monsoon strength started to weaken up to the present day

70 (Overpeck et al., 1996; Dykoski et al., 2005; Wang et al., 2005). Holocene climate
71 change is known to regulate catchment vegetation and soil development,
72 [subsequently influencing aquatic ecosystems](#) (Xiao et al., 2014; Wang et al., 2016a).
73 Major changes in sedimentary diatom assemblages in southwestern China generally
74 correspond with the broad trend of Holocene monsoonal variations, mainly linked
75 to climate-mediated catchment processes (Chen et al., 2014; Li et al., 2015; Wang
76 et al., 2016a; Li et al., 2018).

77 Besides the general trend, Holocene monsoonal variations are characterized by
78 several rapid cooling events in southwestern China lasting several centuries in
79 duration (Hong et al., 2003; Morrill et al., 2003; Mayewski et al., 2004; Wang et al.,
80 2005; Wang et al. 2016b; Ning et al., 2017). Cold events are inferred from lake
81 sediment characteristics such as rapid declines in the proportion of organic matter
82 and changes in grain size and weathering indicators, which suggest an increase in
83 erosion of unweathered material into lake basins (Mischke and Zhang, 2010). Cold
84 events may be associated with prolonged snow-cover, accelerated upland bedrock
85 erosion, and elevated influx of detritus and base cations to the lakes (Koinig et al.,
86 2003; Schmidt et al., 2006; Mischke and Zhang, 2010). Changes in terrestrial
87 [influxes are known to](#) alter limnological conditions and biotic communities in lakes
88 (Likens and Bormann, 1974; Leavitt et al., 2009). However, the effects of Holocene
89 cooling events on alpine lake ecosystems in the monsoon-influenced regions have
90 rarely been assessed.

91 Sedimentary pigments and inorganic elements are analysed from Tiancai Lake,

92 located at treeline in Yunnan Province (SW China). Sedimentary chlorophylls and
93 carotenoids can be used to infer past algal communities (Leavitt and Hodgson, 2001;
94 McGowan, 2013), whereas inorganic elements can provide information about
95 catchment processes such as bedrock erosion and soil formation (Boyle, 2001;
96 Koinig et al., 2003; Schmidt et al., 2006; Lu et al., 2017). This study presents
97 sedimentary element and pigment records in Tiancai Lake over the last 12,000 years,
98 combined with published pollen and diatom data of Tiancai Lake (Chen et al., 2014;
99 Xiao et al., 2014), in order to reveal the linkages between the terrestrial and aquatic
100 ecosystems, and their co-evolution in response to Holocene monsoonal variations.

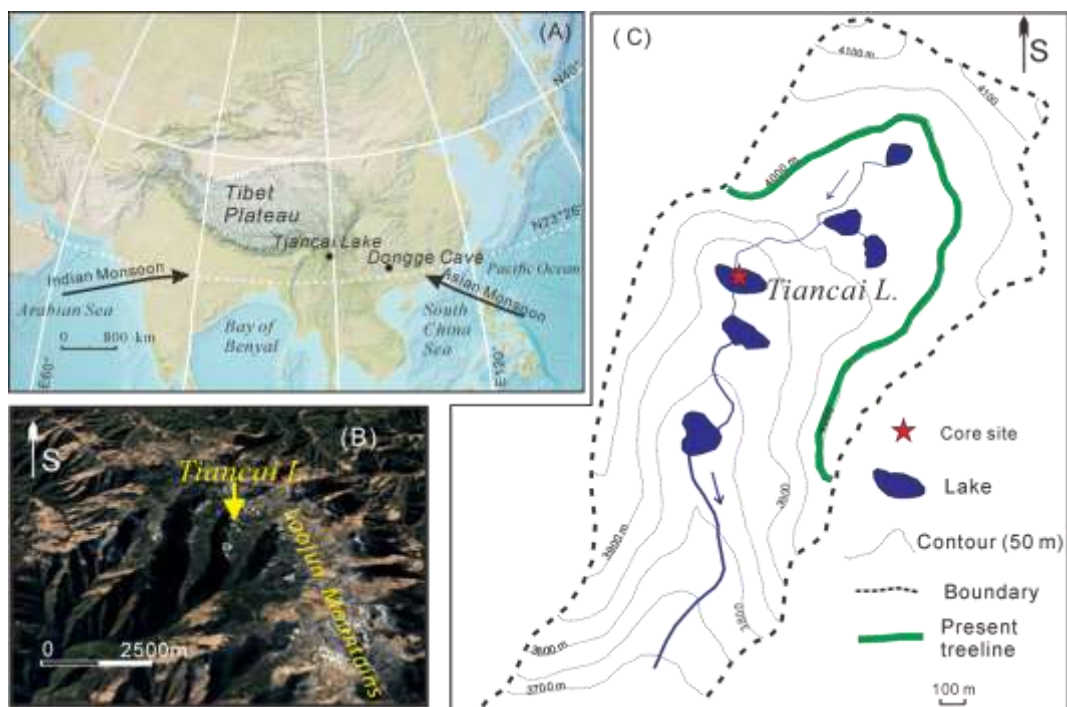
101

102 **2. Materials and methods**

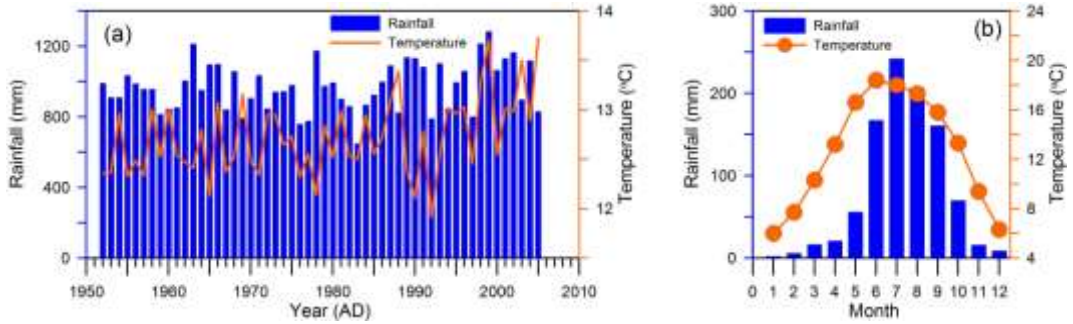
103 2.1. Study area

104 Tiancai Lake (26°38'3.8"N, 99°43'00"E; 3898 m a.s.l.) has a surface area of ~2.1
105 ha, a mean depth of 6 m and is located on granite bedrock at the northeastern slope
106 of the Laojun Mountains (summit ~4200m a.s.l.), which is located at the
107 southeastern edge of the Tibetan Plateau, SW China (Figs. 1A and 1B). **The bedrock**
108 **is characterized by high proportions of SiO₂ (71.3-73.4%) and total alkali**
109 **(K₂O+Na₂O, 7.4-8.8%) (Ma, 2013).** The climate in this region is strongly
110 influenced by the Asian monsoon, with a mean annual temperature of ~12.7°C and
111 mean annual precipitation of ~970 mm at Lijiang City (nearby meteorological
112 station; 2393 m a.s.l.; Fig. 2). Primary forest around the lake appears to be
113 undisturbed, and is characterized by montane conifers such as *Abies georgii*, with

114 the timberline at about 4000 m a.s.l. (Fig. 1C). The upper catchment above the
115 timberline is mainly composed of alpine *Rhododendron* shrubland, *Kobresia*
116 meadow and alpine tundra. Soil type in the catchment is a brown podzolic soil, with
117 a mean pH of 4.03, organic matter of 177 mg g⁻¹, total nitrogen of 11 mg g⁻¹, total
118 phosphorus of 1 mg g⁻¹, total potassium of 10 mg g⁻¹ (Shi, 2007). The lake is
119 hydrologically open with the inflow from the south and an outflow to the north (Fig.
120 1C). The lake water is brown-coloured, with a pH of 7.91, total nitrogen of 0.54 mg
121 L⁻¹, total phosphorus of 14.44 µg L⁻¹, and dissolved organic carbon (DOC) of 10.33
122 mg L⁻¹ measured in June 2013 (Du et al., 2016).



123
124 Figure 1 Maps showing the location of Tiancai Lake in Asia relative to monsoonal
125 pathways (A) and in the Laojun Mountains (B), and topography of Tiancai Lake
126 catchment (C). Maps A and B have been modified from the maps downloaded from
127 <http://www.lib.utexas.edu/maps/asia.html> and Google Earth (imagery captured on
128 December 31, 1994), respectively.



129

130 Figure 2 Mean annual temperature and rainfall (a) and monthly temperature and
 131 rainfall (b) at Lijiang meteorological station (26°52'N, 100°13'E, 2393 m a.s.l.; 56
 132 km away from Tiancai Lake).

133

134 2.2. Sample collection and laboratory analysis

135 A 926 cm long core was extracted from the centre of the lake in 2008 at a water
 136 depth of 6.8 m using a Uwitech Coring Platform System, and sectioned at 1-cm
 137 intervals. Sediments in this core consist of *alternate* dark gyttja and dark silty gyttja,
 138 i.e., black gyttja between 926 and 820 cm, 817 and 692 cm, 587 and 358 cm, 341
 139 and 321 cm, 319 and 96 cm with dark silty gyttja in the intervals; and black gyttja
 140 with many plant remains in the uppermost 96 cm. The age-depth model of Tiancai
 141 Lake is published in Xiao et al. (2014) based on a best-fit second order polynomial
 142 function derived from 18 calibrated radiocarbon dates. In this study, an updated age
 143 model was developed based on the 18 radiocarbon dates using the Bayesian model
 144 (Bacon 2.2) in R language (Blaauw and Christen, 2011). Bacon repeatedly samples
 145 from the probability density function of each calibrated age, fits many possible
 146 splines to the age-depth data, and rejects fitted splines that give rise to age reversals.
 147 Default settings were used when calculating the age-depth model. All ages are
 148 reported in calendar years before radiocarbon present (1950 AD).

149 A total of 100 subsamples taken from the Tiancai Lake core at ~ 10-cm intervals

150 were used for laboratory measurements. For elemental analyses, the freeze dried
151 samples (~125 mg) were completely digested with a mixture of four acids (i.e., HF,
152 HCl, HNO₃ and HClO₄) and prepared for the measurement of Al, Ba, Ca, Sr, Na, K,
153 Mg, Ti, Mn, Fe, P, Pb, Cu and Zn by inductively coupled plasma-atomic emission
154 spectrometry (ICP-AES) with standard solution SPEX™ from the US as the
155 standard (± 2%). Quality control was assured by the analysis of duplicate samples,
156 blanks, and reference materials (GSD-9 and GSD-11, Chinese geological reference
157 materials). The reproducibility of the duplicated sediment samples was >90% for
158 all elements. Blank digestion solution results were <5% for all samples and
159 elements, and all standard deviations in prepared samples were <7% of documented
160 certified values.

161 For pigment analyses, freeze-dried weighed sediments (~200 mg) were extracted in
162 a mixture of acetone: methanol: water (80:15:5) by leaving in a -20°C freezer for
163 24h. Extracts were filtered with a 0.22-µm-pore PTFE filter, dried under N₂ gas, re-
164 dissolved in an acetone: ion-pairing reagent: methanol mixture (70:25:5) and then
165 injected into an Agilent 1200 series high performance liquid chromatography unit
166 (HPLC). The separation conditions with quaternary pump, autosampler, ODS
167 Hypersil column (250×4.6 mm; 5 µm particle size) and photo-diode array detector
168 followed a modification of Chen et al. (2001). Pigments were identified and
169 quantified based on their retention time and absorption spectra, compared with
170 commercial pigment standards from DHI, Denmark (Leavitt and Hodgson, 2001;
171 McGowan, 2013). The analysed pigments included those from all algae and plants

172 (β -carotene, Chl *a*, pheophytin *a*), chlorophytes (Chl *b*, pheophytin *b*, lutein),
173 cyanobacteria (canthaxanthin, zeaxanthin), siliceous algae (diatoxanthin) and
174 cryptophytes (alloxanthin). Lutein and zeaxanthin did not separate in this study and
175 so were reported here together. All concentrations were expressed as nmol⁻¹ g
176 organic carbon.

177

178 2.3. Data analysis

179 The chemical index of alteration (CIA) was used to evaluate the weathering
180 intensity of minerals in the sediment (Nesbitt and Young, 1982).

$$181 \quad \text{CIA} = \frac{\text{Al}_2\text{O}_3}{(\text{Al}_2\text{O}_3 + \text{K}_2\text{O} + \text{Na}_2\text{O} + \text{CaO})} \times 100$$

182 where elemental abundances are expressed as molar proportions. A CIA value of
183 100 indicates intense chemical weathering along with complete removal of all the
184 alkali (oxidation state +1) and alkaline (oxidation state +2) earth elements, whereas
185 CIA values of 45-55 indicate less weathering.

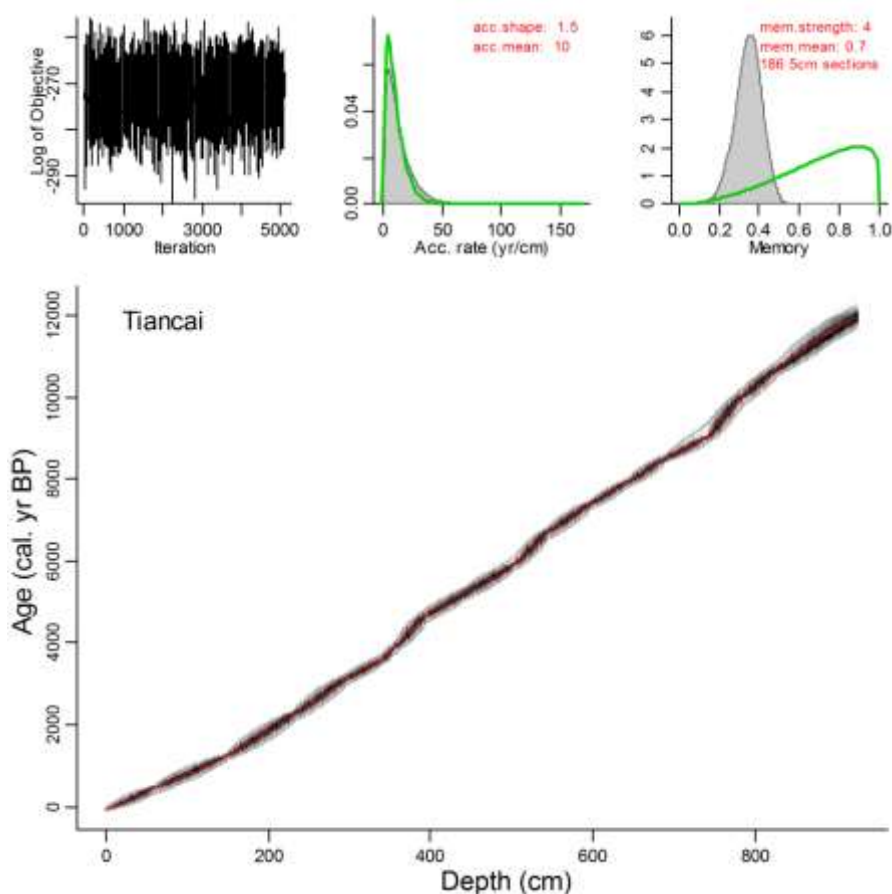
186 Zonation schemes were developed for pigments and elements using the broken-
187 stick model (Bennett, 1996) using stratigraphically constrained cluster analysis
188 (CONISS) in the Tilia program (Grimm, 1991). Principal components analysis
189 (PCA) was used to summarise the major underlying changes in each stratigraphical
190 dataset because the gradient lengths of both pigment and element data, as assessed
191 by earlier detrended correspondence analysis (DCA), were less than 1 standard
192 deviation (Šmilauer and Lepš, 2014). Ordination analyses were performed on log
193 ($x+1$)-transformed pigment data and square-root transformed element data.

194 In order to understand the driving forces for environmental changes in Tiancai Lake,
195 pigment and element data were compared with previously published datasets,
196 including sedimentary records from Tiancai Lake: median grain size, magnetic
197 susceptibility (χ_{lf}), TN, TOC, *Aulacoseira alpigena* (diatom) relative abundance and
198 the percentage of *Tsuga* (pollen) (Han et al., 2011; Chen et al., 2014, Xiao et al.,
199 2014); and global climatic records: Dongge Cave $\delta^{18}\text{O}$ values (Dykoski et al., 2005),
200 hematite-stained grain in the eastern North Atlantic (Bond et al., 2001), potassium
201 ion content proxy from Greenland ice cores at GIPS2 (Mayewski et al., 2004),
202 detrended decadal atmospheric $\Delta^{14}\text{C}$ (Stuiver et al., 1998), Ti records from the
203 Cariaco Basin (Haug et al., 2001), Greenland ice-core (NGRIP) $\delta^{18}\text{O}$ records
204 (Rasmussen et al., 2006), and average summer insolation at 30°N (Berger and
205 Loutre, 1991).

206 Redundancy analysis (RDA) was conducted to evaluate the relationship between
207 pigments/elements and explanatory variables from the abovementioned datasets. In
208 addition, sediment depth was added as an explanatory variable in order to assess the
209 influence of lake infilling on environmental changes of Tiancai Lake. Forward
210 selection, with the false discovery rate (FDR) correction, and Monte Carlo tests (p
211 < 0.05 , $n = 499$ unrestricted permutations) were used to determine a minimum
212 subset of explanatory variables. All ordinations were performed using CANOCO
213 5.0 (Šmilauer and Lepš, 2014).

214

215 **3. Results**



217

218 Figure 3 Age-depth model for Tiancai Lake. Grayscale cloud represents age model
 219 probability and is bounded by a dotted-line confidence interval (95%); the darkest
 220 grey colour indicates the highest probability age for that depth. The red line shows
 221 the weighted mean age-depth model.

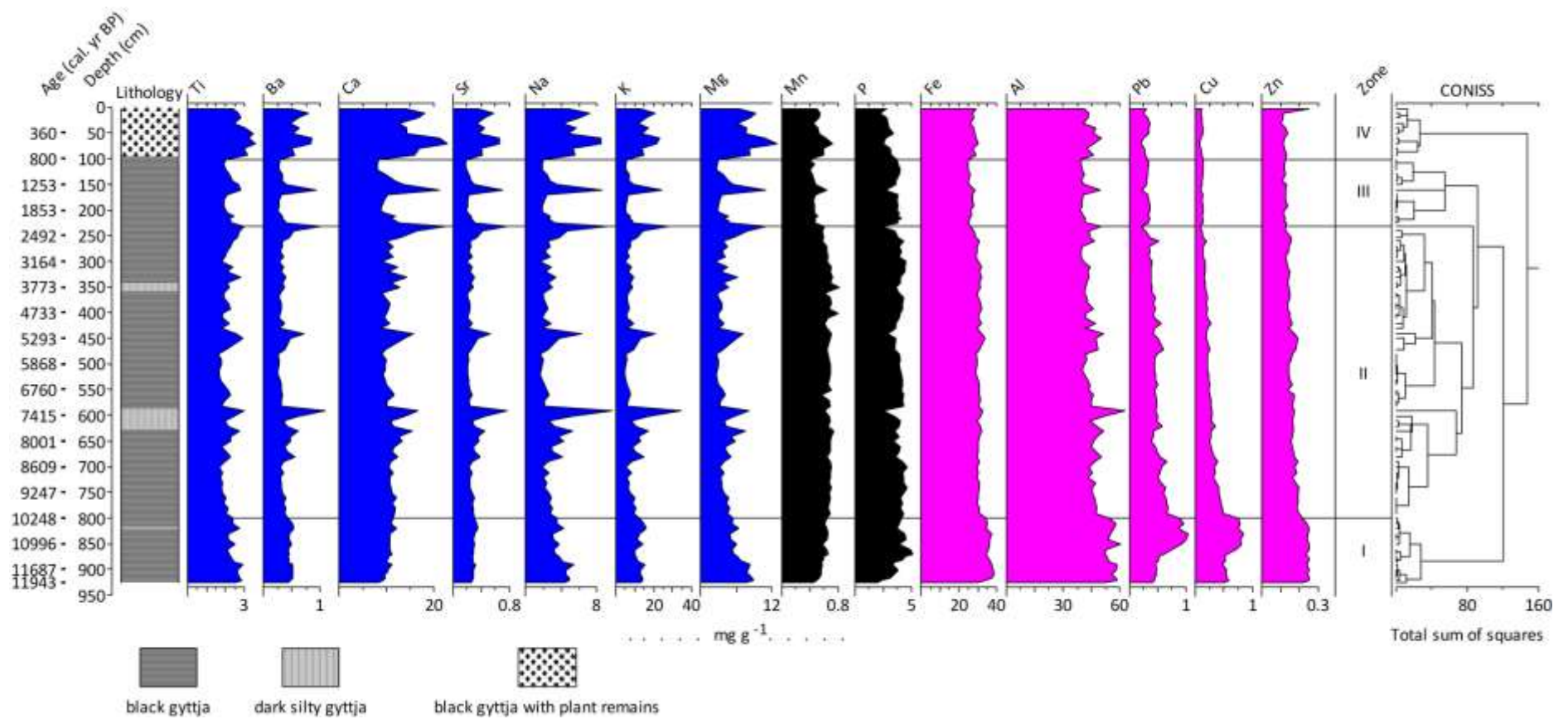
222 The relationship between age and depth is shown in Fig.3. The basal age of the core
 223 is ca. 11943 ± 261 cal. yr BP. The sedimentation rate in Tiancai Lake core is rather
 224 uniform, with a mean value of ca. 0.77 mm/yr. Comparison of the Bayesian model
 225 (produced in Bacon) with the polynomial fitted model (Xiao et al., 2014), shows
 226 that they are in close alignment ($R=0.999$, $p<0.001$). The average temporal
 227 resolution for pigment and element samples is ~119 years.

228

229 3.2. Sedimentary elements

230 Three distinct trends are observed in the element record (Fig. 4). Concentrations of
231 Fe, Al, Pb, Cu and Zn were highly correlated ($r > 0.53$) and showed general
232 declining trends after temporary increases at the bottom of the core. The second
233 group consists of Ti, Ba, Ca, Sr, Na, K and Mg, which were strongly correlated ($r >$
234 0.71) and displayed high fluctuations, especially in the mid-to-late Holocene. Mn
235 and P increased in the [early Holocene stages](#) and retained high values in the mid-
236 Holocene, followed by decreasing trends in the late Holocene.

237 [Stratigraphic element concentrations](#) were split into four significant zones indicated
238 by CONISS (Fig. 4). Zone I (925-801 cm; 11943-10263 [cal. yr BP](#)) was
239 characterized by the highest levels of Fe, Al, Pb, Cu and Zn. Concentrations of Ti,
240 Na, K and Mg declined, and Mn and P concentrations increased. Concentrations of
241 Ba, Ca and Sr were quite stable. In Zone II (801-232 cm; 10263-2245 [cal. yr BP](#)),
242 Al, Pb, Cu and Zn declined whereas there were several synchronous peaks in Ti,
243 Ba, Ca, Sr, Na, K and Mg centred at around 8390, 7773, 7297, 5191, 3491 and 2245
244 [cal. yr BP](#), respectively. Concentrations of Mn, P and Fe maintained relatively high
245 values, with slight fluctuations.



246

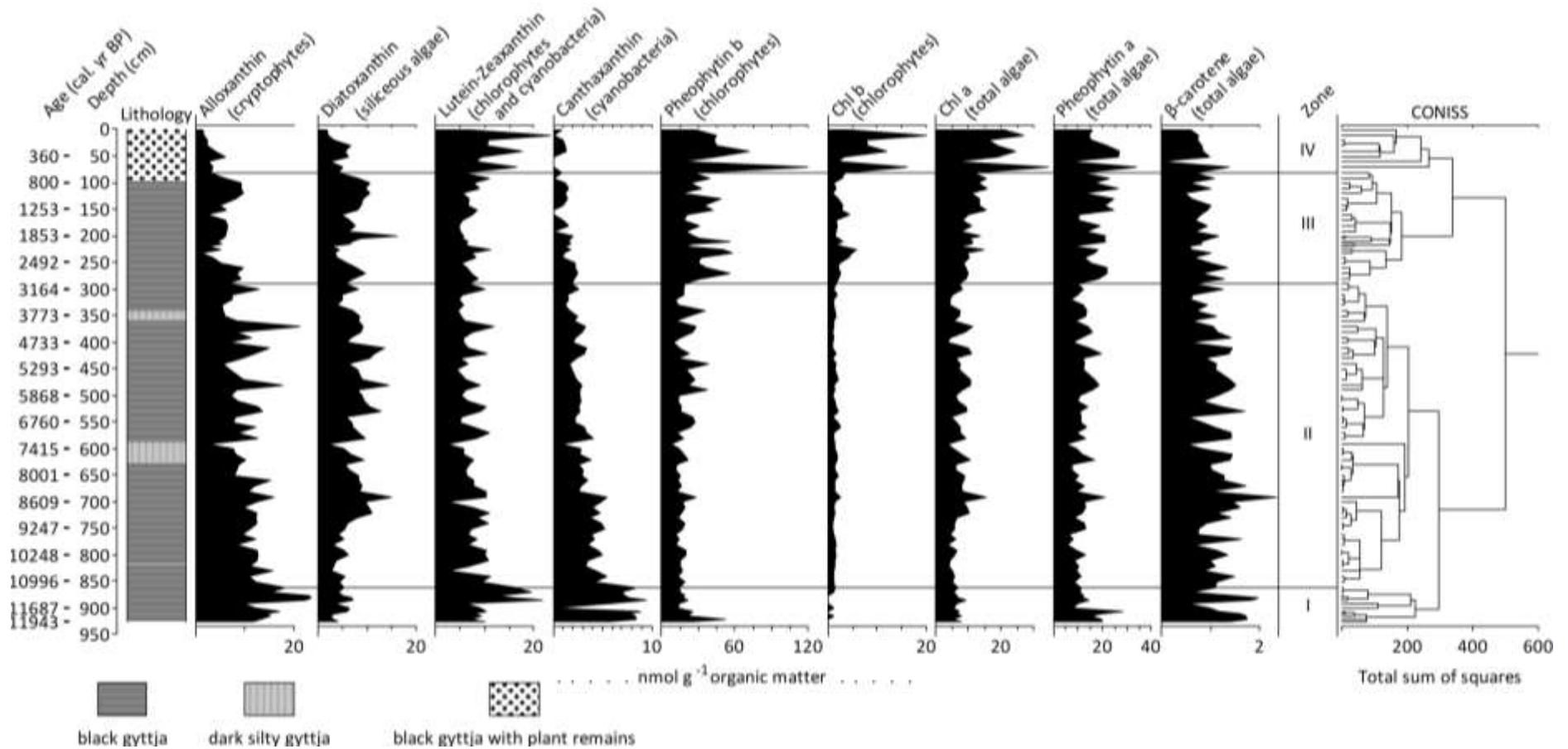
247 Figure 4 Sedimentary element concentrations for the Tiancai Lake core. The number of statistically significant zones was assessed using the broken
 248 stick model (Bennett, 1996).

249 In Zone III (232-102 cm; 2245-817 cal. yr BP), Ti, Ba, Ca, Sr, Na, K, Mg and Al
250 were variable, with one synchronous peak centred at around 1385 cal. yr BP,
251 accompanied by two troughs in P. Mn and Fe declined obviously, while Pb, Cu and
252 Zn retained low concentrations. In Zone IV (102-0 cm; 817 cal. yr BP to present),
253 concentrations of Ti, Ba, Ca, Sr, Na, K and Mg increased to high levels, with one
254 synchronous peak centred at around 541 cal. yr BP. Pb, Cu and Zn were relatively
255 stable and retained low values. P showed a declining trend, while Mn, Fe and Al
256 increased slightly in comparison with Zone III.

257

258 3.3. Sedimentary pigments

259 CONISS divided the stratigraphic pigment record into four zones (Fig. 5). In Zone
260 I (925-861 cm; 11943-11152 cal. yr BP) the cryptophyte pigment alloxanthin was
261 abundant, and maximum abundance of the cyanobacterial pigment canthaxanthin
262 was recorded alongside. High abundances of lutein-zeaxanthin (from chlorophytes
263 and cyanobacteria) and β -carotene (ubiquitous in algae but often particularly
264 abundant in cyanobacteria) were observed. In contrast, pigments from chlorophytes
265 (Chl *b*, pheophytin *b*) and siliceous algae (diatoxanthin) were present in low
266 abundances and concentrations of pigments from all algae (Chl *a*, pheophytin *a*)
267 were moderate.



268

269

270

Figure 5 Fossil pigment diagram of the Tiancai Lake core, with pigment affinity given in parentheses. The number of statistically significant zones was assessed using the broken stick model (Bennett, 1996).

271 In Zone II (861-291 cm; 11152-3054 cal. yr BP) concentrations of pigments from
272 cryptophytes (alloxanthin) and cyanobacteria (canthaxanthin and zeaxanthin)
273 decreased slightly, but those from siliceous algae and all algae (β -carotene, Chl *a*
274 and pheophytin *a*) increased with a notable maximum at around 8500 cal. yr BP.
275 Pigments from chlorophytes (Chl *b* and pheophytin *b*) displayed no directional trend.
276 Zone III (291-81 cm; 3054-631 cal. yr BP) was characterized by increasing
277 concentrations of chlorophylls and derivatives, including Chl *b* and pheophytin *b*
278 (from chlorophytes) and Chl *a* and pheophytin *a* (from all primary producers). The
279 abundance of diatoxanthin from siliceous algae was variable but high, whereas there
280 were decreases in cyanobacteria (canthaxanthin) and cryptophytes (alloxanthin).

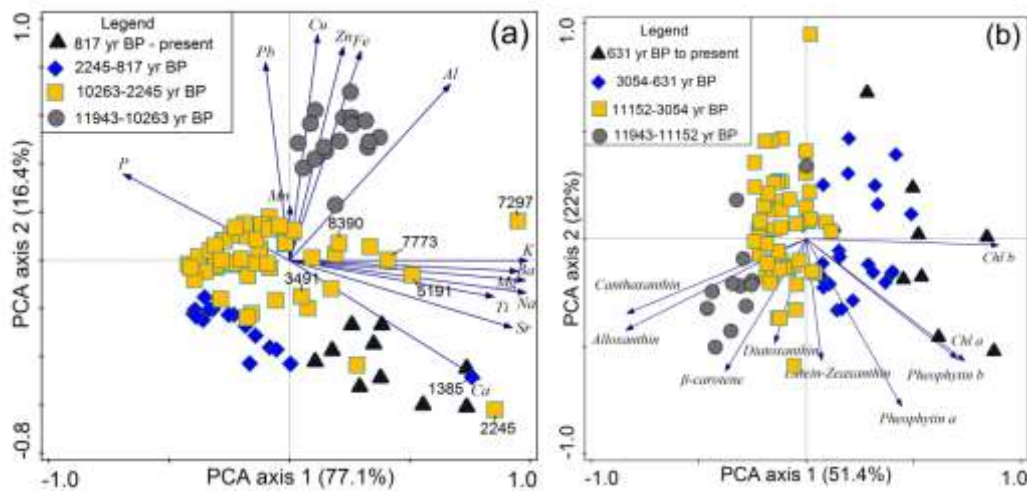
281 In Zone IV (81-0 cm; 631 cal. yr BP to present) pigment assemblages were
282 markedly different from other zones. Concentrations of chlorophytes and total algal
283 pigments were much higher (Chls *a* and *b*, pheophytins *a* and *b*), and abundances
284 of pigments from siliceous algae (diatoxanthin), cryptophytes (alloxanthin) and
285 cyanobacteria (canthaxanthin) were lower.

286

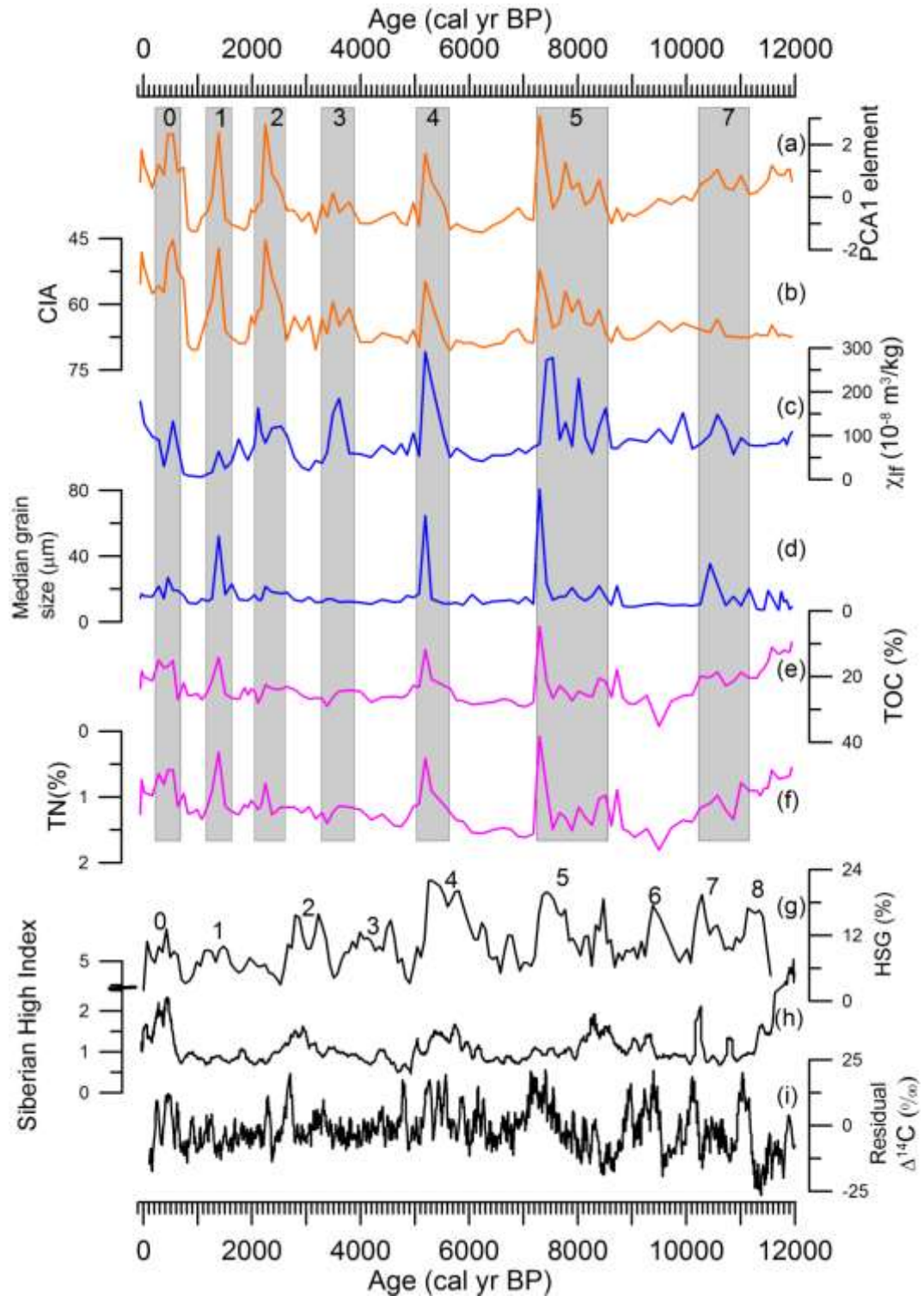
287 3.4. Multivariate analysis

288 For the elemental data, the first two PCA axes captured 93.5% of the total variance
289 (Fig. 6a). PCA axis 1 (PCA1_{elements}) was positively correlated with K, Mg, Ba, Na,
290 Ti, Sr and Ca, while PCA axis 2 (PCA2_{elements}) was positively related to Cu, Pb, Zn,
291 Fe, Al and Mn (Fig. 6a). For pigments, PCA axis 1 (PCA1_{pigments}) explained 51.4%
292 of the total variance and was strongly correlated with chlorophylls and their

293 derivatives from chlorophytes (Chl *b* and pheophytin *b*) and all primary producers
 294 (Chl *a* and pheophytin *a*) (Fig. 6b). PCA axis 2 (PCA2_{pigments}) explained a further
 295 22% of the variance in the pigment assemblages and was correlated with
 296 carotenoids from chlorophytes/cyanobacteria (lutein-zeaxanthin), siliceous algae
 297 (diatoxanthin), cyanobacteria (canthaxanthin) and cryptophytes (alloxanthin).



298
 299 Figure 6 Principal components analyses of elements (four zones correspond to those
 300 in Figure 4; a) and pigments (four zones correspond to those in Figure 5; b). Cold
 301 events are labelled with their age in Fig. 6a.



302

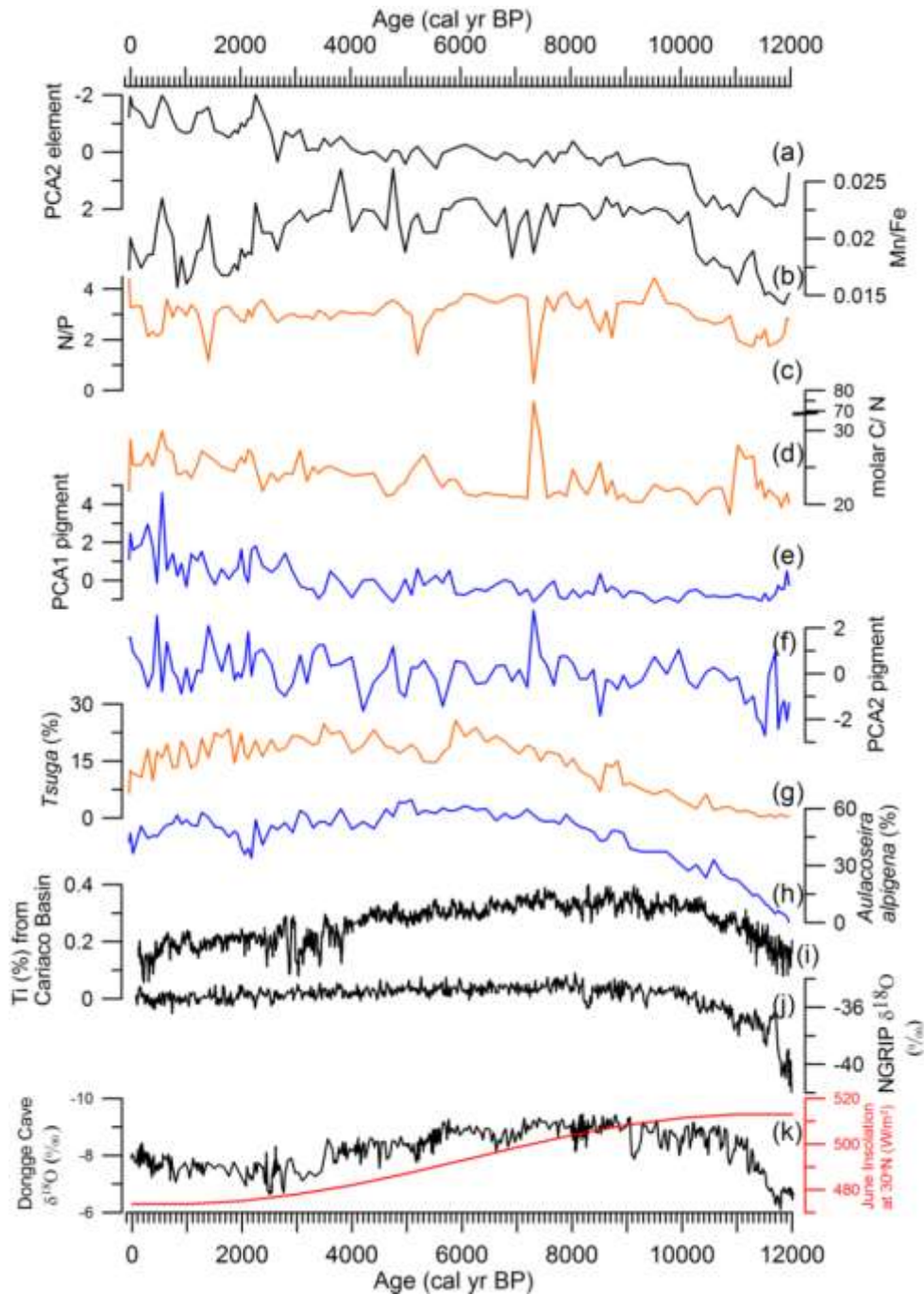
303 Figure 7 Short-term oscillations in sedimentary proxies from Tiancai Lake (a-f) in
 304 comparison with global climatic records (g-i). (a) Element sample scores on PCA
 305 axis 1; (b) chemical index of alteration (CIA); (c) magnetic susceptibility (Han et
 306 al., 2011); (d) median grain size (Han et al., 2011); (e) total organic carbon (Chen
 307 et al., 2014); (f) total nitrogen (Chen et al., 2014), expressed on the timescale used
 308 in this study. (g) Hematite-stained grain (%) in the eastern North Atlantic (MC52-
 309 VM29-191; Bond et al., 2001). (h) Siberian High index based on potassium ion

310 content (K^+ ; ppb) proxy from Greenland ice cores at GIPS2 after an adjacent-
311 averaging smoothing (100 yr) (Mayewski et al., 2004). (i) Detrended decadal
312 atmospheric $\Delta^{14}C$ (Stuiver et al., 1998). The grey bars indicate the timing of seven
313 Bond-like cooling events during the Holocene.

314

315 $PCA1_{elements}$ correlated with CIA, median grain size, magnetic susceptibility, TOC
316 and TN (Figs. 7a-f). In addition, seven visible oscillations in physical and
317 geochemical records of Tiancai Lake can be correlated within the radiocarbon age
318 uncertainties to the North Atlantic cooling events (Fig. 7g).

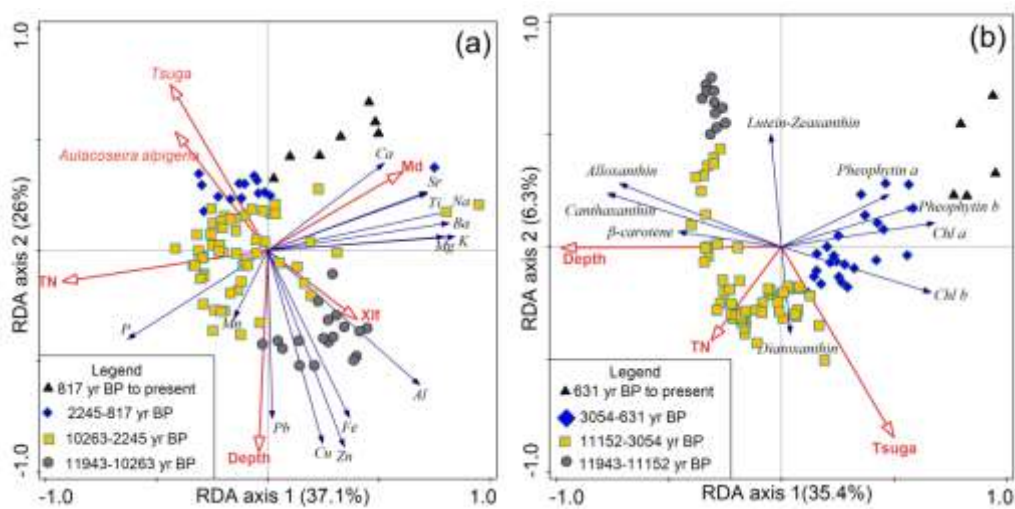
319 $PCA2_{elements}$ showed a declining trend, whereas $PCA1_{pigments}$ increased gradually
320 (Figs. 8a and 8e). Mn/Fe ratio increased in the early Holocene, maintained high
321 values in the middle Holocene, and declined in the late Holocene (Fig. 8b). The
322 broad trend in Mn/Fe is paralleled by major changes in tree pollen (*Tsuga*), diatom
323 species (*A. alpigena*), the Cariaco Basin Ti records and Dongge Cave $\delta^{18}O$ values
324 (Fig. 8).



325
 326 Figure 8 Long-term changes in sedimentary proxies from Tiancai Lake (a-h) in
 327 comparison with global climatic records (i-k). (a) Element sample scores on PCA2;
 328 (b) the ratios of manganese to iron (Mn/Fe); (c) the ratios of nitrogen to phosphorus
 329 (N/P); (d) the molar ratios of carbon to nitrogen (C/N); (e) pigment sample scores
 330 on PCA 1; (f) pigment sample scores on PCA 2; (g) percentage of *Tsuga* in pollen
 331 assemblage (Xiao et al., 2014); (h) percentage of *A. alpigena* in diatom assemblage
 332 (Chen et al., 2014), expressed against the age-depth model used in this study. (i) Ti
 333 records from the Cariaco Basin (Haug et al., 2001). (j) Greenland ice-core (NGRIP)
 334 $\delta^{18}\text{O}$ records (Rasmussen et al., 2006). (k) D4 $\delta^{18}\text{O}$ record from Dongge Cave and
 335 average summer insolation at 30°N (Black: Dykoski et al., 2005; red: Berger and
 336 Loutre, 1991).

337

338 RDA results revealed that changes in elemental composition were significantly
339 correlated with median grain size (Md), magnetic susceptibility (χ_{lf}), *Tusga*, *A.*
340 *alpigena* and TN in Tiancai lake core, as well as sediment depth (Fig. 9a).
341 Meanwhile, *Tsuga*, TN and sediment depth formed the minimum subset of
342 significant variables for explaining the variance in pigment data (Fig. 9b).



343

344 Figure 9 Biplot of redundancy analysis, (a) elements and significant explanatory
345 variables (four zones correspond to those in Figure 4) and (b) elements and
346 significant explanatory variables (four zones correspond to those in Figure 5).

347

348 4. Discussion

349 4.1. Catchment soil formation

350 Low TOC and TN contents but high concentrations of minerogenic elements in the
351 basal samples probably reflected the organically poor and mineral-rich soil in the
352 alpine meadow around Tiancai Lake before ~11 ka BP. High P concentration in the
353 early part of the record (before ~ 10 ka BP) might have resulted from rich leachable
354 P (e.g., apatite) and high supply rate of P from the treeless catchment (cf. Boyle,

2007). Since ~ 10 ka BP, evergreen trees expanded in montane regions (SW China) due to the intensified summer monsoon, suggested by rising *Tsuga* percentage in the pollen records from Tiancai Lake (Xiao et al., 2014), Lugu Lake (Wang et al., 2016a) and Chenghai Lake (Xiao et al., 2017). Forest development can stabilize soils and gradually reduce inorganic inputs to lakes (Ford, 1990; Hu et al., 1993). For instance, the mobilization of Al, Pb, Cu and Zn from soil A horizons would occur during soil podsolization, with these elements typically deposited lower in the soil profile forming a spodic horizon (cf. Ford, 1990). As a consequence of declining supply from the catchment, Al, Pb, Cu and Zn decreased progressively in lake sediments after ~10 ka BP.

Meanwhile, increased litter fall from trees would have increased soil humic content, elevated soil acidity, and decreased soil aeration (Hu et al., 1993). Under anoxic conditions, both Mn and Fe may be expected to become mobilized and to pass into solution; a more rapid reduction of Mn than Fe causes preferential Mn release (Mackereth, 1966; Naeher et al., 2013). Increasing Mn/Fe ratios from the early- to mid- Holocene [could be linked to](#) preferential removal of Mn from catchment soils, probably due to the onset of reducing conditions in the soils of sufficient intensity to produce Mn²⁺ but not intense enough to generate Fe²⁺ (Mackereth, 1966). Due to strengthened monsoon intensity since the early Holocene, faster lake flushing and so less bottom water anoxia could account for increasing Mn/Fe ratios further (Naeher et al., 2013). In addition, sedimentary P retained relatively high values for several thousand years (from ~10 to 2 ka BP), probably resulting from high

377 sedimentation efficiency from co-precipitation with oxidizing Fe and Mn within
378 lake and biological sedimentation by phytoplankton (Mackereth, 1966).
379 Sedimentary phosphorus content in Tiancai Lake (ranging from 1.98 to 5.14 mg g⁻
380 ¹) is relatively higher than that in other lakes of Yunan Province (ranging from 0.68
381 to 2.1 mg g⁻¹) (Whitmore et al., 1997).
382 Declining TN and TOC contents after ~ 3 ka BP implied soil thinning due to forest
383 retreat (Xiao et al., 2014), which will in turn weaken reducing conditions in
384 catchment soils and limit the migration of Fe and Mn, revealed by general decreases
385 in Fe and Mn. Besides the general trend, several peaks in Mn/Fe ratios were likely
386 linked to the separation of Fe and Mn during erosional transport (cf. Mackereth,
387 1966). PCA 2_{elements} was positively correlated with Al, Pb, Cu and Zn, Mn, Fe and
388 P (Fig. 6a), indicating that PCA 2_{elements} mainly reflect surrounding soil development.
389

390 4.2. Episodic erosion events

391 Synchronous peaks in minerogenic elements (i.e., Ti, Ba, Ca, Sr, Na, K and Mg),
392 median grain size and magnetic susceptibility coincided with troughs in CIA values
393 (Figs. 4 and 7), indicative of high intensity of freeze-thaw processes that removed
394 unleached and coarse detritus materials before the processes of chemical attack had
395 time to be fully effective (Mackereth, 1966; Boyle, 2001). These erosion events,
396 likely linked to prolonged ice-cover and ice-melt duration in the catchment
397 (Schmidt et al., 2006), could transport detritus materials **directly** into the lake by
398 meltwater inflow and slope wash (Pennington et al., 1972; Solovieva and Jones,

399 2002). Positive correlations between PCA 1_{element} and these minerogenic elements
400 suggested that PCA 1_{element} mainly represent the erosion intensity of upland bedrock.
401 These strong erosion events, within dating error, can be correlated with Holocene
402 cold events recorded in lake sediments, peats and ice cores from the Tibetan Plateau
403 and adjacent montane regions (see the review by Mischke and Zhang, 2010), as well
404 as Holocene ice-rafting events in the North Atlantic (Fig. 7g). For example, the cold
405 spell between 8.5 and 7.2 ka BP was inferred also from other sites located in the
406 eastern Tibetan Plateau, including Hongyuan Peatland (Hong et al., 2003), Naleng
407 Lake (Kramer et al., 2010) and Ximencuo Lake (Mischke and Zhang, 2010). The
408 cold events in the North Atlantic region, which resulted from changes in external
409 solar forcing (Wang et al., 2005) and internal oceanic and atmospheric circulation
410 (Darby et al., 2012), could influence the East Asian winter monsoon probably
411 through the impact of the Siberian High (Gong et al., 2001; Fig. 7h). In addition,
412 the orographically-derived features of the Tibetan Plateau (e.g., an extended snow-
413 cover period) and catchment-specific response (e.g., steep topography) of the lake
414 system could enhance the impacts of these cold events (Kramer et al., 2010;
415 Mischke and Zhang, 2010; Anderson et al., 2012). For instance, the steep and
416 rugged topography of the Tiancai Lake catchment could facilitate upland bedrock
417 weathering by the freeze-thaw process because of the sharp gradients in climatic
418 parameters (e.g., temperature and radiation) over very short distances (Brisset et al.,
419 2014). Future investigation is needed to assess the linkage between these cold
420 events and other atmospheric processes, such as El Niño-Southern Oscillation

421 (ENSO) events.

422

423 4.3. Changes in algal community structure

424 High abundances of cyanobacteria and cryptophytes during the early Holocene
425 were positively correlated with sediment depth (Fig. 9b), indicating that they may
426 be influenced by lake water depth; sediment infilling has gradually reduced lake
427 depth by ca. 9 m over the last 12 ka. Both cyanobacteria and cryptophytes are suited
428 to deeper lakes which stratify, due to their ability to alter their depth position in the
429 water column to optimise access to nutrients (P and N). Cyanobacteria are also
430 particularly prevalent in alkaline environments, with abundant minerals and
431 phosphorus from the treeless catchment (McGowan et al., 2008; Reuss et al., 2010).
432 In addition, they are known to be well suited to cold environments (Leavitt and
433 Findlay, 1994; Lotter, 2001).

434 With vegetation and soil development from ca. 11 ka BP, microbial nitrogen fixation
435 in soils would be enhanced by early successional plants (Fritz et al., 2004), such as
436 *Alnus* around Tiancai Lake (Xiao et al., 2014). After nitrogen mineralization during
437 winter, substantial inorganic nitrogen is exported from terrestrial systems during the
438 snowmelt season, when terrestrial plants are unable to utilize the plant available N
439 pool (Fritz and Anderson, 2013). Increasing nitrogen supply, suggested by rising
440 TN contents and N/P ratios (Figs. 7f and 8c), would favour siliceous algae over
441 cyanobacteria in the lake (Cross et al., 2014; Fig 9b). Meanwhile, an increasing
442 influx of dissolved organic matter from terrestrial sources, indicated by rising TOC

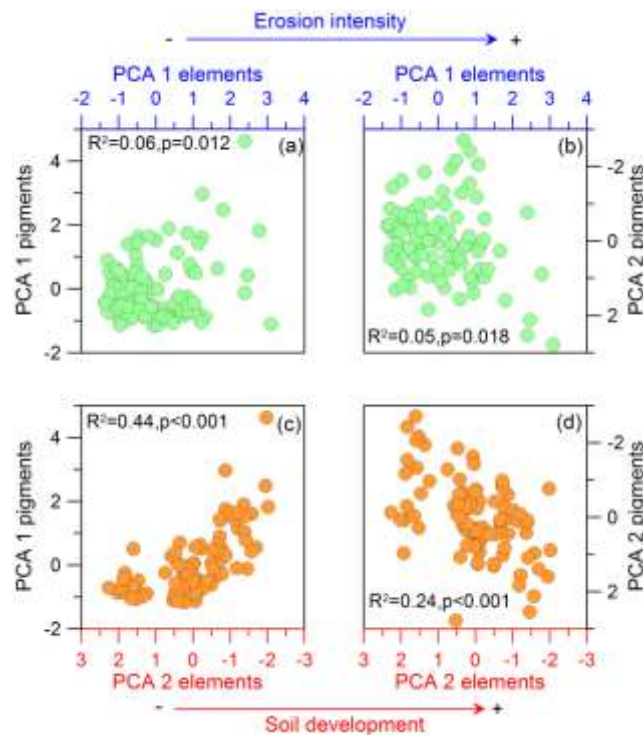
443 content, might have reduced the light availability and alkalinity of the lake water
444 (Williamson et al., 1999; Engstrom et al., 2000). Such conditions are highly suited
445 to cryptophytes, which persisted at this time as they are able to employ mixitrophy
446 to utilise organic carbon sources (Lepistö and Rosenström, 1998). Cryptophytes and
447 other siliceous algae groups such as chrysophytes are common in dystrophic lakes
448 (Jones et al., 2011). Despite a weakening of the monsoon intensity after the mid-
449 Holocene (Dykoski et al., 2005), no directional trends in pigment concentrations
450 indicated relatively stable algal communities for the timespan from ~7 to 3 ka BP,
451 probably due to replete supplies of phosphorus and nitrogen.

452 The most marked transition around 3 ka BP, i.e., substantial increases in pigments
453 from chlorophyte/ higher plants and obvious decreases in cyanobacteria and
454 cryptophytes, signified a major ecological shift in Tiancai Lake. A return to
455 relatively dry and cold climatic conditions in the late Holocene led to the
456 replacement of trees (*Tsuga*) by shrubs (Ericaceae) and surface runoff reduction in
457 the catchment (Chen et al., 2014; Xiao et al., 2014). As a consequence, reducing
458 tree canopy in the littoral zone and declining supply of terrestrial organic matter to
459 the lake could increase light penetration depths. Coupled with increasingly
460 shallower lake depths due to sediment infilling, this probably expanded benthic
461 production in the lake. Accordingly the pigments indicate increased production of
462 (benthic) chlorophytes, or aquatic macrophytes (each indicated by the pigments Chl
463 *b* and pheophytin *b*) (Reuss et al., 2010). A slight increase in C/N ratios after ~3 ka
464 BP (Fig. 8d) probably indicated a rising contribution of macrophytes (Meyers and

465 Ishiwatari, 1993). Further increase in Chl *b* and pheophytin *b* after ~ 541 yr BP
466 denoted favourable light and nutrient conditions for chlorophytes, since the vast
467 majority of chlorophytes are autotrophic (Wehr et al., 2015).

468

469 4.4. The links between catchment and lake processes



470

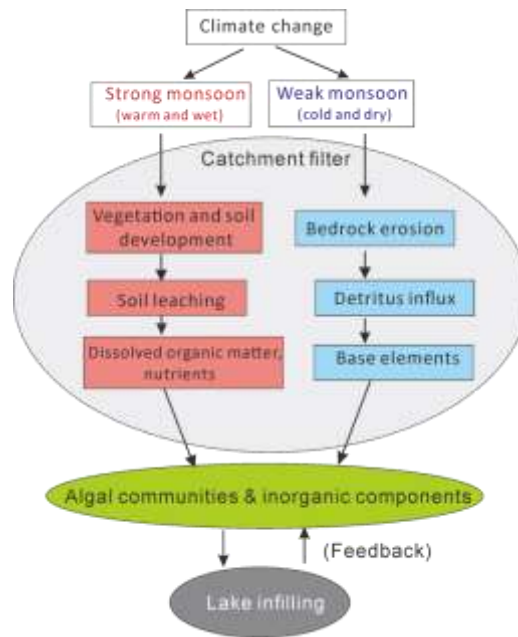
471 Figure 10 Correlation relationships between pigment and element data, including
472 PCA1_{elements} and PCA 1_{pigments} (a), PCA 1_{elements} and PCA 2_{pigments} (b), PCA 2_{elements}
473 and PCA 1_{pigments} (c), and PCA 2_{elements} and PCA 2_{pigments} (d).

474

475 Both pigment and elemental data were significantly correlated with TN (catchment
476 soil), *Tsuga* (vegetation) and sediment depth (lake infilling) (Figs. 9a-b),
477 highlighting direct and indirect effects of Holocene monsoonal variations on lake
478 ecosystem evolution. For instance, the peaks of minerogenic elements (i.e., Ti, Ba,
479 Ca, Sr, Na, K and Mg) mainly responded to prolonged ice-cover period and
480 enhanced physical weathering during cold events, while the decrease in

481 cyanobacteria was partly linked to lake infilling since the early Holocene. Despite
482 several erosion events in Tiancai Lake catchment, there are subtle responses of algal
483 communities to these erosion processes, suggested by weak correlations between
484 pigment data and PCA 1_{elements} (an indicator for erosion intensity; Figs. 10a-b). In
485 contrast, pigment data were highly correlated with PCA 2_{elements} (a proxy for soil
486 development; Figs. 10c-d). The results denoted that direct responses of algae to
487 short-term climatic oscillations are overridden by strong catchment-lake
488 interactions. Specifically, in this region where sources of P (from bedrock
489 weathering) and N (from soil development) have been replete for much of the
490 Holocene, there are only subtle changes in overall primary producer abundance,
491 with the most marked effects later in the record being caused by internal (lake
492 infilling) processes.

493 During cold events, clastic materials are produced by bedrock weathering and
494 transported annually in the lake by melt-waters in the spring (Fig. 11). Meanwhile,
495 percolation of melt-water through paludified soil supplied solutes (e.g., phosphorus
496 and nitrogen) to this lake, helping to maintain relatively stable limnological
497 conditions for algae during the growth season (Catalan et al., 2013). Feedback
498 mechanisms operate effectively whereby changes in limnological conditions (e.g.,
499 an increase in alkalinity) due to strong erosion can be inhibited by buffering
500 processes in catchment soils (Fig. 11).



501

502 Figure 11 Representation of catchment and lake processes in response to Holocene
 503 monsoonal variations.

504

505 In addition, both element and pigment data were significantly correlated with
 506 sediment depth, highlighting the strong influence of lake infilling on the lake. The
 507 natural progressive infilling due to gradual accumulation of terrestrial and
 508 autochthonous materials leads to lake shallowing and littoral zone expansion,
 509 conforming to models of lake ontogeny (Binford et al 1983). As a consequence, the
 510 development of benthic chlorophytes and aquatic macrophytes contributed to the
 511 increases in Chl *b* and pheophytin *b* in the late Holocene. Meanwhile, lake volume
 512 loss would shorten water retention time, indirectly altering sedimentation rate and
 513 redox condition in water column. Hence, lake infilling could interact with climatic
 514 variations and catchment processes, influencing phytoplankton community and
 515 geochemical processes in Tiancai Lake.

516

517 **5. Conclusion**

518 Sedimentary pigments and elements in Tiancai Lake were analysed to reveal the co-
519 evolution of catchment and lake ecosystems in response to Holocene monsoonal
520 variations. High abundances of cyanobacteria and cryptophytes in the early
521 Holocene were related to alkaline conditions after the deglaciation, and relatively
522 stable algal communities in the mid-Holocene was followed by the expansion of
523 chlorophytes and/ or aquatic plants in the late Holocene. Al, Zn, Cu and Pb
524 decreased generally from the early Holocene, mainly in response to catchment soil
525 development. Changes in Mn and Fe were related to redox condition dynamics in
526 catchment soils and water column. Peaks in Ti, Ba, Ca, Sr, Na, K and Mg signified
527 erosion events and the influxes of unleached particles and base cations. Despite
528 several erosion events, the rather subtle variations in algal communities were
529 probably linked to replete nutrient supply from catchment soils. The catchment can
530 filter the direct effects of climate on lakes, because local bedrock, topography, soils
531 and vegetation alter runoff and mass transfer from land to water. Overall, this study
532 provides well-dated pigment and element records in an alpine lake during the
533 Holocene, underscoring strong co-evolutionary relationships between climate,
534 vegetation, soil development, lake infilling and algal communities.

535

536 **Acknowledgements**

537 We thank Teresa Needham, Graham Morris, Qianglong Qiao and Yuxin Zhu for
538 help with laboratory analyses. This work was supported by National Key R&D

539 Program of China (2016YFA0600501), the National Natural Science Foundation of
540 China (41572149, 41572343), and the Fundamental Research Fund for National
541 University, China University of Geosciences (Wuhan) (G1323511656). Xu Chen
542 was supported by a Postdoctoral Scholarship of the China Scholarship Council
543 (201206415008).

544

545 **References**

546 Anderson, N. J., A. C. Liversidge, S. McGowan & M. D. Jones, 2012. Lake and catchment response
547 to Holocene environmental change: spatial variability along a climate gradient in southwest
548 Greenland. *J. Paleolimn.* 48(1):209-222

549 Battarbee, R., R. Thompson, J. Catalan, J.-A. Grytnes & H. J. B. Birks, 2002. Climate variability
550 and ecosystem dynamics of remote alpine and arctic lakes: the MOLAR project. *J. Paleolimn.*
551 28(1):1-6

552 Bennett, K. D., 1996. Determination of the number of zones in a biostratigraphical sequence. *New*
553 *Phytol.* 132(1):155-170

554 Berger, A. & M. F. Loutre, 1991. Insolation values for the climate of the last 10000000 years. *Quat.*
555 *Sci. Rev.* 10(4):297-317

556 Blaauw, M. & J. A. Christen, 2011. Flexible paleoclimate age-depth models using an autoregressive
557 gamma process. *Bayesian Anal.* 6(3):457-474

558 Binford, M.W., E.S. Deevey & T.L. Crisman, 1983. Paleolimnology: an historical perspective
559 on lacustrine ecosystems. *Ann. Rev. Ecol. Syst.* 14(1): 255-286.

560 Bond, G., B. Kromer, J. Beer, R. Muscheler, M. N. Evans, W. Showers, S. Hoffmann, R. Lotti-Bond,

561 I. Hajdas & G. Bonani, 2001. Persistent Solar Influence on North Atlantic Climate During the
562 Holocene. *Science* 294(5549):2130-2136.

563 Boyle, J., R. Chiverrell, A. Plater, I. Thrasher, E. Bradshaw, H. Birks & J. Birks, 2013. Soil mineral
564 depletion drives early Holocene lake acidification. *Geology* 41(4):415-418.

565 Boyle, J. F., 2001. Inorganic Geochemical Methods in Palaeolimnology. In Last, W. M. & J. P. Smol
566 (eds) *Tracking Environmental Change Using Lake Sediments: Physical and Geochemical Methods*.
567 Springer Netherlands, Dordrecht, 83-141.

568 Boyle, J. F., 2007. Loss of apatite caused irreversible early-Holocene lake acidification. *Holocene*
569 17(4):543-547

570 Bradshaw, E. G., V. J. Jones, H. J. B. Birks & H. Birks, 2000. Diatom responses to late-glacial and
571 early-Holocene environmental changes at Kråkenes, western Norway. *J. Paleolimn.* 23(1):21-34

572 Brisset, E., C. Miramont, F. Guiter, E. J. Anthony, K. Tachikawa, J. Poulencard, F. Arnaud, C. Delhon,
573 J.-D. Meunier, E. Bard & F. Suméra, 2013. Non-reversible geosystem destabilisation at 4200 cal.
574 BP: Sedimentological, geochemical and botanical markers of soil erosion recorded in a
575 Mediterranean alpine lake. *Holocene* 23(12):1863-1874

576 Catalan, J., S. Pla-Rabés, A. Wolfe, J. Smol, K. Rühland, N. J. Anderson, J. Kopáček, E. Stuchlík,
577 R. Schmidt, K. Koinig, L. Camarero, R. Flower, O. Heiri, C. Kamenik, A. Korhola, P. Leavitt, R.
578 Psenner & I. Renberg, 2013. Global change revealed by palaeolimnological records from remote
579 lakes: a review. *J. Paleolimn.* 49(3):513-535

580 Chen, N., T. S. Bianchi, B. A. McKee & J. M. Bland, 2001. Historical trends of hypoxia on the
581 Louisiana shelf: application of pigments as biomarkers. *Org. Geochem.* 32(4):543-561

582 Chen, X., Y. Li, S. Metcalfe, X. Xiao, X. Yang & E. Zhang, 2014. Diatom response to Asian monsoon

583 variability during the Late Glacial to Holocene in a small treeline lake, SW China. *Holocene*
584 24(10):1369-1377.

585 Cross, I. D., S. McGowan, T. Needham & C. M. Pointer, 2014. The effects of hydrological extremes
586 on former gravel pit lake ecology: management implications. *Fundam. Appl. Limnol.* 185(1):71-
587 90

588 Darby, D. A., J. D. Ortiz, C. E. Grosch & S. P. Lund, 2012. 1,500-year cycle in the Arctic Oscillation
589 identified in Holocene Arctic sea-ice drift. *Nat. Geosci.* 5(12):897-900

590 Du, Y., Y. Zhang, F. Chen, Y. Chang & Z. Liu, 2016. Photochemical reactivities of dissolved organic
591 matter (DOM) in a sub-alpine lake revealed by EEM-PARAFAC: An insight into the fate of
592 allochthonous DOM in alpine lakes affected by climate change. *Sci. Total Environ.* 568:216-225

593 Dykoski, C. A., R. L. Edwards, H. Cheng, D. X. Yuan, Y. J. Cai, M. L. Zhang, Y. S. Lin, J. M. Qing,
594 Z. S. An & J. Revenaugh, 2005. A high-resolution, absolute-dated Holocene and deglacial Asian
595 monsoon record from Dongge Cave, China. *Earth Planet. Sci. Lett.* 233(1-2):71-86

596 Engstrom, D. R., S. C. Fritz, J. E. Almendinger & S. Juggins, 2000. Chemical and biological trends
597 during lake evolution in recently deglaciated terrain. *Nature* 408(6809):161-166

598 Ford, M. S., 1990. A 10 000-Yr History of Natural Ecosystem Acidification. *Ecol. Monogr.* 60(1):57-
599 89

600 Fritz, S. C. & N. J. Anderson, 2013. The relative influences of climate and catchment processes on
601 Holocene lake development in glaciated regions. *J. Paleolimn.* 49(3):349-362

602 Fritz, S. C., D. R. Engstrom & S. Juggins, 2004. Patterns of early lake evolution in boreal landscapes:
603 a comparison of stratigraphic inferences with a modern chronosequence in Glacier Bay, Alaska.
604 *Holocene* 14(6):828-840.

605 Gong, D.Y., S.W. Wang & J.H. Zhu, 2001. East Asian Winter Monsoon and Arctic Oscillation.
606 Geophys. Res. Lett. 28(10):2073-2076

607 Grimm, E., 1991. TILIA version 1.11. TILIAGRAPH version 1.18. A Users Notebook Illinois State
608 Museum, Springfield, USA.

609 Han, Y., X. Xiao, X. Yang, E. Zhang & J. Y. Xiao, 2012. The grain-size characteristics of Tiancai
610 Lake in northwestern of Yunnan Province and paleo-precipitation history during the Holocene.
611 Quat. Res. 31:999-1010 (in Chinese).

612 Haug, G. H., K. A. Hughen, D. M. Sigman, L. C. Peterson & U. Röhl, 2001. Southward Migration
613 of the Intertropical Convergence Zone Through the Holocene. Science 293(5533):1304-1308.

614 Hong, Y. T., B. Hong, Q. H. Lin, Y. X. Zhu, Y. Shibata, M. Hirota, M. Uchida, X. T. Leng, H. B.
615 Jiang, H. Xu, H. Wang & L. Yi, 2003. Correlation between Indian Ocean summer monsoon and
616 North Atlantic climate during the Holocene. Earth Planet. Sci. Lett. 211(3 - 4):371-380

617 Hu, F. S., L. B. Brubaker & P. M. Anderson, 1993. A 12000 year record of vegetation change and
618 soil development from Wien Lake, central Alaska. Can. J. Bot. 71(9):1133-1142

619 Jones, V.J., Solovieva, N., Self, A.E., McGowan, S., Rosen, P., Salonen, J.S., Seppä, H., Valiranta,
620 M., Parrott, E. & Brooks, S.J. 2011. The influence of Holocene tree-line advance and retreat on an
621 arctic lake ecosystem: a multi-proxy study from Kharinei Lake, North Eastern European Russia.
622 Journal of Paleolimnology 46(1), 123-137.

623 Koinig, K. A., W. Shotyk, A. F. Lotter, C. Ohlendorf & M. Sturm, 2003. 9000 years of geochemical
624 evolution of lithogenic major and trace elements in the sediment of an alpine lake – the role of
625 climate, vegetation, and land-use history. J. Paleolimn. 30(3):307-320

626 Kramer, A., U. Herzschuh, S. Mischke & C. Zhang, 2010. Holocene treeline shifts and monsoon

627 variability in the Hengduan Mountains (southeastern Tibetan Plateau), implications from
628 palynological investigations. *Palaeogeogr. Palaeoclimatol. Palaeoecol.* 286(1):23-41

629 Leavitt, P. & D. Hodgson, 2001. Sedimentary Pigments. In Smol, J., H. J. Birks, W. Last, R. Bradley
630 & K. Alverson (eds) *Tracking Environmental Change Using Lake Sediments. Developments in*
631 *Paleoenvironmental Research*, vol 3. Springer Netherlands, 295-325.

632 Leavitt, P. R. & D. L. Findlay, 1994. Comparison of fossil pigments with 20 years of phytoplankton
633 data from eutrophic Lake-227, experimental lakes area, Ontario. *Can. J. Fish. Aquat. Sci.*
634 51(10):2286-2299

635 Leavitt, P. R., S. C. Fritz, N. J. Anderson, P. A. Baker, T. Blenckner, L. Bunting, J. Catalan, D. J.
636 Conley, W. O. Hobbs, E. Jeppesen, A. Korhola, S. McGowan, K. Ruhland, J. A. Rusak, G. L.
637 Simpson, N. Solovieva & J. Werne, 2009. Paleolimnological evidence of the effects on lakes of
638 energy and mass transfer from climate and humans. *Limnol. Oceanogr.* 54(6):2330-2348.

639 Lepistö, L. & Rosenström, U. 1998. The most typical phytoplankton taxa in four types of boreal
640 lakes. *Hydrobiologia* 369(0), 89-97.

641 Li, Y., E. Liu, X. Xiao, E. Zhang & M. Ji, 2015. Diatom response to Asian monsoon variability
642 during the Holocene in a deep lake at the southeastern margin of the Tibetan Plateau. *Boreas*
643 44(4):785-793.

644 Li, Y., X. Chen, X. Xiao, H. Zhang, B. Xue, J. Shen & E. Zhang, 2018. Diatom-based inference of
645 Asian monsoon precipitation from a volcanic lake in southwest China for the last 18.5 ka. *Quat.*
646 *Sci. Rev.* 182:109-120

647 Likens, G. E. & F. H. Bormann, 1974. Linkages between Terrestrial and Aquatic Ecosystems.
648 *Bioscience* 24(8):447-456

649 Lotter, A., 2001. The palaeolimnology of Soppensee (Central Switzerland), as evidenced by diatom,
650 pollen, and fossil-pigment analyses. *J. Paleolimn.* 25(1):65-79

651 Lotter, A. F. & H. J. B. Birks, 2003. The Holocene palaeolimnology of Sägistalsee and its
652 environmental history – a synthesis. *J. Paleolimn.* 30(3):333-342

653 Lu, Y., S. C. Fritz, J. R. Stone, T. R. Krause, C. Whitlock, E. T. Brown & J. V. Benes, 2017. Trends
654 in catchment processes and lake evolution during the late-glacial and early- to mid-Holocene
655 inferred from high-resolution XRF data in the Yellowstone region. *J. Paleolimn.* 58(4):551-569

656 Ma, H.H. 2013. Petrology and geochemical characteristics of Laojunshan Granite in southeast
657 Yunnan and its tectonic significance. Master thesis. China University of Geosciences (Beijing),
658 Beijing, China (in Chinese).

659 Mackereth, F. J. H., 1966. Some Chemical Observations on Post-Glacial Lake Sediments. *Philos. T.*
660 *R. Soc. B* 250(765):165-213.

661 Mayewski, P. A., E. E. Rohling, J. C. Stager, W. Karlen, K. A. Maasch, L. D. Meeker, E. A. Meyerson,
662 F. Gasse, S. van Kreveld, K. Holmgren, J. Lee-Thorp, G. Rosqvist, F. Rack, M. Staubwasser, R. R.
663 Schneider & E. J. Steig, 2004. Holocene climate variability. *Quat. Res.* 62(3):243-255

664 McGowan, S., 2013. PALEOLIMNOLOGY | Pigment Studies. In Elias, S. A. & C. J. Mock (eds)
665 *Encyclopedia of Quaternary Science (Second Edition)*. Elsevier, Amsterdam, 326-338.

666 McGowan, S., R. K. Juhler & N. J. Anderson, 2008. Autotrophic response to lake age, conductivity
667 and temperature in two West Greenland lakes. *J. Paleolimn.* 39(3):301-317

668 Meyers, P. A. & R. Ishiwatari, 1993. Lacustrine organic geochemistry—an overview of indicators
669 of organic matter sources and diagenesis in lake sediments. *Org. Geochem.* 20(7):867-900

670 Mischke, S. & C. Zhang, 2010. Holocene cold events on the Tibetan Plateau. *Global Planet. Change*

671 72(3):155-163

672 Morrill, C., J. T. Overpeck & J. E. Cole, 2003. A synthesis of abrupt changes in the Asian summer
673 monsoon since the last deglaciation. *Holocene* 13(4):465-476

674 Naeher, S., A. Gilli, R. P. North, Y. Hamann & C. J. Schubert, 2013. Tracing bottom water
675 oxygenation with sedimentary Mn/Fe ratios in Lake Zurich, Switzerland. *Chem. Geol.* 352:125-
676 133

677 Nesbitt, H. W. & G. M. Young, 1982. Early proterozoic climates and plate motions inferred from
678 major element chemistry of lutites. *Nature* 299(5885):715-717.

679 Ning, D., E. Zhang, W. Sun, J. Chang & J. Shulmeister, 2017. Holocene Indian Summer Monsoon
680 variation inferred from geochemical and grain size records from Lake Ximenglongtan,
681 southwestern China. *Palaeogeogr. Palaeoclimatol. Palaeoecol.* 487:260-269

682 Overpeck, J., D. Anderson, S. Trumbore & W. Prell, 1996. The southwest Indian Monsoon over the
683 last 18000 years. *Clim. Dynam.* 12(3):213-225

684 Pennington, W., T. G. Tutin, E. Haworth, A. P. Bonny & J. P. Lishman, 1972. Lake Sediments in
685 Northern Scotland. *Philos. T. R. Soc. B* 264(861):191-294

686 Rasmussen, S. O., K. K. Andersen, A. M. Svensson, J. P. Steffensen, B. M. Vinther, H. B. Clausen,
687 M. L. Siggaard-Andersen, S. J. Johnsen, L. B. Larsen, D. Dahl-Jensen, M. Bigler, R. Röthlisberger,
688 H. Fischer, K. Goto-Azuma, M. E. Hansson & U. Ruth, 2006. A new Greenland ice core
689 chronology for the last glacial termination. *J. Geophys. Res. Atmos.* 111(D6):

690 Renberg, I., 1990. A 12600 Year Perspective of the Acidification of Lilla Oresjon, Southwest
691 Sweden. *Philos. T. R. Soc. B* 327(1240):357-361.

692 Reuss, N. S., D. Hammarlund, M. Rundgren, U. Segerstrom, L. Eriksson & P. Rosen, 2010. Lake

693 Ecosystem Responses to Holocene Climate Change at the Subarctic Tree-Line in Northern Sweden.
694 Ecosystems 13(3):393-409

695 Schmidt, R., C. Kamenik, R. Tessadri & K. A. Koinig, 2006. Climatic changes from 12,000 to 4,000
696 years ago in the Austrian Central Alps tracked by sedimentological and biological proxies of a lake
697 sediment core. J. Paleolimn. 35(3):491-505

698 Shi, J.P. 2007. Community ecology and biogeography of the mossy dwarf forest in Yunan. PhD
699 thesis. Xishuangbanna Tropical Botanical Garden, Chinese Academy of Sciences, Kunming,
700 China (in Chinese).

701 Šmilauer, P. & J. Lepš, 2014. Multivariate Analysis of Ecological Data using CANOCO 5, 2 ed.
702 Cambridge University Press, Cambridge.

703 Solovieva, N. & V. J. Jones, 2002. A multiproxy record of Holocene environmental changes in the
704 central Kola Peninsula, northwest Russia. J. Quat. Sci. 17(4):303-318

705 Stuiver, M., P. J. Reimer, E. Bard, J. W. Beck, G. S. Burr, K. A. Hughen, B. Kromer, G. McCormac,
706 J. Van der Plicht & M. Spurk, 1998. INTCAL98 radiocarbon age calibration, 24,000-0 cal BP.
707 Radiocarbon 40(3):1041-1083.

708 Wang, Q., X. Yang, N. J. Anderson & X. Dong, 2016a. Direct versus indirect climate controls on
709 Holocene diatom assemblages in a sub-tropical deep, alpine lake (Lugu Hu, Yunnan, SW China).
710 Quat. Res. 86(1):1-12

711 Wang, X., G. Chu, M. Sheng, S. Zhang, J. Li, Y. Chen, L. Tang, Y. Su, J. Pei & Z. Yang, 2016b.
712 Millennial-scale Asian summer monsoon variations in South China since the last deglaciation.
713 Earth Planet. Sci. Lett. 451:22-30

714 Wang, Y., H. Cheng, R. L. Edwards, Y. He, X. Kong, Z. An, J. Wu, M. J. Kelly, C. A. Dykoski & X.

715 Li, 2005. The Holocene Asian Monsoon: Links to Solar Changes and North Atlantic Climate.
716 Science 308(5723):854-857

717 Wehr, J. D., R. G. Sheath & J. P. Kociolek, 2015. Freshwater algae of North America: ecology and
718 classification. Elsevier.

719 Williamson, C. E., D. P. Morris, M. L. Pace & O. G. Olson, 1999. Dissolved organic carbon and
720 nutrients as regulators of lake ecosystems: Resurrection of a more integrated paradigm. Limnol.
721 Oceanogr. 44(3):795-803.

722 Whitmore, T.J., Brenner, M., Jiang, Z., Curtis, J.H., Moore, A.M., Engstrom, D.R. and Wu, Y. 1997.
723 Water quality and sediment geochemistry in lakes of Yunnan Province, southern China.
724 Environmental Geology 32(1), 45-55.

725 Xiao, X., S. G. Haberle, Y. Li, E. Liu, J. Shen, E. Zhang, J. Yin & S. Wang, 2017. Evidence of
726 Holocene climatic change and human impact in northwestern Yunnan Province: High-resolution
727 pollen and charcoal records from Chenghai Lake, southwestern China. Holocene 28(1): 127-139.

728 Xiao, X., S. G. Haberle, J. Shen, X. Yang, Y. Han, E. Zhang & S. Wang, 2014. Latest Pleistocene
729 and Holocene vegetation and climate history inferred from an alpine lacustrine record,
730 northwestern Yunnan Province, southwestern China. Quat. Sci. Rev. 86(0):35-48

731 Zhang, E., J. Chang, Y. Cao, W. Sun, J. Shulmeister, H. Tang, P. G. Langdon, X. Yang & J. Shen,
732 2017. Holocene high-resolution quantitative summer temperature reconstruction based on
733 subfossil chironomids from the southeast margin of the Qinghai-Tibetan Plateau. Quat. Sci. Rev.
734 165:1-12